Outstanding performance of the microwave-made MMO-Ti/RuO₂IrO₂ anode on the removal of antimicrobial activity of Penicillin G by photoelectrolysis

Isabelle M.D. Gonzaga[a,b,c], Angela Moratalla[c], Katlin I. B. Eguiluz[a,b], Giancarlo R. Salazar-Banda[a,b], Pablo Cañizares[c], Manuel A. Rodrigo[c], Cristina Saez[c,*]

a Electrochemistry and Nanotechnology Laboratory, Research and Technology Institute - ITP, Aracaju, SE, Brazil

b Processes Engineering Post-graduation - PEP, Universidade Tiradentes, 49037-580 Aracaju, SE, Brazil

c Chemical Engineering Department, Universidad de Castilla-La Mancha, Campus Universitario, Ciudad Real, Spain

[*] Author to whom all correspondence should be addressed (cristina.saez@uclm.es)

ABSTRACT: This paper studies the applicability of a novel microwave-prepared mixed metal oxide (MMO-Ti/RuO$_2$IrO$_2$) anode in the electrolysis and photo-electrolysis of synthetic urine intensified with Penicillin G. Results are compared with those obtained using boron-doped diamond (BDD) as the anode. In general, electrolysis with both anodes are effective in terms of penicillin removal, and the combination with UV radiation shows a clear synergistic effect on the degradation of Penicillin G: 420% and 355% using MMO and BDD, respectively. The outstanding performance of the MMO-Ti/RuO$_2$IrO$_2$ anode is demonstrated by the decrease in toxicity and the reduction of the antibiotic effect on the urine observed during photo-electrolysis. Notably, photo-electrolysis using the MMO-Ti/RuO$_2$IrO$_2$ anode generates solutions with almost zero residual toxicity and without antibiotic effect, with lower specific energy consumption than using BDD anode. The remarkable performance of the microwaves-prepared MMO-Ti/RuO$_2$IrO$_2$ coatings makes them very promising for being used in the electrochemical treatment of sanitary wastes.

Keywords: Photo-electrochemical; mixed metal oxide; diamond electrode; toxicity; antibiotic activity.

1. Introduction

The development of anodes with outstanding physical and chemical stability and low cost has become a key aspect in the design of cost-effective electrochemical advanced oxidation processes. Two types are the most studied [1] and consist of coatings of mixed metal oxide anodes (MMO) or boron-doped diamond (BDD) deposited on different substrates. It has been proposed that the first type is suitable for use in combination with other technologies because of its associated low oxygen evolution potential, which mainly allows the conversion of organic pollutants into other more oxidizable compounds, in particular carboxylic acids [2–5]. The second type has excellent properties and can achieve complete mineralization because they have high oxygen evolution potential, which is strategic for the complete oxidation of organics to CO_2 and H_2O [6–8]. The essential difference between both types is the cost, and the lower cost of MMO anodes has attracted the interest of many researchers.

MMO anodes consist of mixtures of two or more metal oxides that form new stable compounds that show significant improvements in catalytic activity and stability relative to their respective single-component metal oxides [9]. Their excellent electrocatalytic properties have led to their use in the Chlor-alkali industry [10] and oxygen and hydrogen production by electrolysis in water [11]. Because of its excellent mechanical stability, long service life, and electrocatalytic activity, RuO_2–IrO_2 is one of the most promising candidates for a highly efficient MMO anode [12,13] as an electrocatalyst in electrochemical systems [14,15]. In a previous study conducted by our research group [16], the new anode (MMO-Ti/RuO_2IrO_2) made using hybrid microwave heating was reported. In that study, physical and electrochemical characterizations were performed, whereas accelerated life tests at a current density of 1 A cm^{-2} in an H_2SO_4 1.0 mol L^{-1} solution were applied to estimate the stability of the anode. It was observed that the new anode has improved properties and

maintained a constant potential for 350 h in these harsh conditions. However, they are less efficient in the oxidation of organic matter than BDD anodes [17]. Therefore, research focus on seeking a combination of technologies to use them in potential applications for wastewater. At this point, many studies have focused on the use of electro-oxidation in combination with other oxidation technologies, such as ultraviolet (UV) radiation [18], ultrasound (US) [19], or the Fenton process [6]. Among them, it is known that UVC radiation allows us to generate higher concentrations of free radicals from the photo-activation of the electrogenerated oxidants [20], resulting in a high synergistic effect [21]. Additionally, it minimizes the typical mass transfer limitations found in diluted wastewater electrolysis [22].

Therefore, the development of stable and efficient MMO anodes has become a top priority [23]. In this context, this work aims to study the feasibility of using a special type of MMO-Ti/RuO_2IrO_2 anode made by using a microwave technique [24] for the electrolysis and photo-electrolysis comparing the results reached with those obtained using commercial BDD anodes (the most well-known anodes). Because of the tremendous potential applicability, a particular case of study has been proposed: the treatment of synthetic urine polluted with antibiotic Penicillin G. Urine is a complex matrix where drugs (and their metabolites) are concentrated and its management in hospitals is a key point to prevent diffusion of antibiotic-resistant bacteria. Results will help to understand the behavior of the MMO-Ti/RuO_2IrO_2 anode in a complex matrix in which inorganic and organic compounds compete for oxidation, and they will also help to elucidate the use of such electrodes to transform potentially hazardous pharmaceutics into other less hazardous intermediate compounds. Additionally, it will contribute to design effective management to reduce the impact of hospital wastewater on the environment and health.

4

2. Experimental

2.1 Chemicals

In this study, urine was used as a supporting electrolyte, and its composition was previously reported elsewhere [5]. Urine consists of a mixture of organic species such as urea, creatinine, uric acid, and inorganic salts (including potassium chloride, magnesium sulfate, or diammonium hydrogen phosphate). Thus, the urine was polluted with 50 mg dm^{-3} of Penicillin G (PenG) to assess the degradation of the antibiotic in this medium. The antibiotic under study and the organic compounds present in the urine were purchased from Sigma Aldrich were of analytical grade (99%). High purity water (Millipore Milli-Q system, resistivity> 18 MΩ) was used to prepare all solutions. The High-performance liquid chromatography (HPLC) mobile phase (Methanol and formic acid) reagents were purchased from Sigma-Aldrich and were of analytical grade.

2.2 Experimental set-up

All experiments were carried out in a conventional single compartment cell, with three electrodes and a capacity of 150 mL with pH maintained at 5.9 (natural pH of urine) and controlled temperature at 25ºC. The working electrode (WE) (4 cm^2 of geometric area) was MMO-Ti/RuO$_2$IrO$_2$ prepared with hybrid microwave heating, using a domestic microwave from Consul (700 W and 2.45 GHz). A box of insulating bricks and SiC slabs were used to obtain homogeneous and porous surfaces, and the synthesis temperature was set at 350 ºC. The heating was maintained until the electrodes reached a mass of around 1.2 mg cm^{-2} [16,24]. The counter electrode was a platinum wire. Ag/AgCl was used as a reference electrode. The electrode gap between the anode and the cathode was 1.0 cm. For comparison purposes, a commercial boron-doped diamond (BDD - supplied by Adamant Technologies) was also used as WE. An Autolab PGSTAT302N (Metrohm - Pensalab) was used to provide

current, and applied current density was set at 30 mA cm^{-2}. A UVC lamp (254 mm, 9 W) was immersed in the tank to carry out the photolysis and photoelectrolysis tests.

2.3 Analytical

The total organic carbon (TOC) concentration was monitored using a TOC analyzer Multi N/C 3100 Analytik Jena. Chemical oxygen demand (COD) analyses were conducted by using a Spectroquant® test CSB from Merck. The Penicillin G concentration was quantified by HPLC (Agilent 1260 series), equipped with an Eclipse Plus C-18 column (4.6mm × 100mm; 3.5 µm). The mobile phase was a mixture of 50% methanol and 50% formic acid (0.1%) at a flow rate of 0.6 mL min^{-1}. The wavelength for detection was 220 nm. The injection volume was 20.0 µL, the column temperature was set to 30 °C, and the retention time was 2.4 min. The intermediates were identified on an Agilent 1260 Infinity coupled to an Agilent time-of-flight mass spectrometer (LC-MS TOF 6230). The mobile phase, composed of 50% methanol and 50% aqueous solution with 0.1% formic acid, flowed at 0.6 mL min^{-1} through a Zorbax Eclipse Plus C-18 column (4.6 mm × 100 mm; 3.5 µm). The injection volume was 10 µL. The mass spectrometer was operated at positive electrospray ionization under the following conditions: capillary, 3500 V; drying gas, 10.0 L/min; gas temperature, 325 ºC; nebulizer 50 psi; skimmer voltage, 65 V. In addition, the evolution of organic compounds present in the urine composition was monitored using HPLC (uric acid), ion chromatography (creatinine), and colorimetric methods (urea) according to the previously reported methodologies [8].

2.4 Synergistic coefficient

The synergistic coefficient (%) was calculated [25] using Eq. (1), where k is the kinetic constant calculated for the different single and combined processes studied (electrolysis, photo-electrolysis, and photolysis).

$$\text{Synergy coefficient } (\%) = \frac{k_{Photoelectro} - k_{electro} - k_{photo}}{k_{photo} + k_{electro}} \; x \; 100 \qquad (1)$$

2.5 Specific energy consumption

According to Eq. (2), was calculated the specific energy consumption (SEC), where I is the current (in A), V is the solution volume (L), E_{cell} is the average cell voltage (V), $PenG_0$ is the initial concentration of the drug, $PenG_t$ is the concentration at a selected time, and t is the time in hours [26].

$$SEC = \frac{E_{cell} \, I \, t}{V \, (PenG_{o-} \, PenG_t)} \qquad (2)$$

2.6 Toxicity

To better understand the processes used, the acute toxicity of the effluents was evaluated using the marine bacterium *Vibrio Fisheri*. The inhibition of bacterial bioluminescence was measured following the procedure indicated by the manufacturer (Microtox®). The samples were analyzed after exposure to the bacteria for 5 and 15 min and compared with the reference sample.

2.7 Antibiotic activity assay

Additionally, the residual antibiotic activity of the treated samples was monitored by counting the number of microorganisms with a μ-Trac® 4200 (Sy-lab, Austria). Initially, the microorganisms were placed on plates with agar and incubated at 37 °C for 24 hours. Subsequently, the urine matrix was contaminated with 10^6–10^7 CFU of *Enterococcus*

7

faecalis, and a blank sample was measured to control the initial concentration of microorganisms. The treated samples were then added to the blank matrix (containing *E. Faecalis*) in four different concentrations (1, 1:10, 1:100, and 1:1000) and kept under agitation for 3 hours at 37 °C. Finally, CFU was quantified by μ-Trac® 4200.

3. Results and discussion

Firstly, to obtain a complete view of the characteristics of the materials, scanning electron microscopy (SEM) and cyclic voltammetry (CVs) were performed (Fig.1). Figs 1a and 1b show the SEM images of the anodes prepared. Note that the MMO coating surface (Fig. 1a) is highly porous and homogeneous. It is attributed to the novel preparation method that employs microwave irradiation for heating. In the case of BDD, smaller crystals are observed (Fig. 1b). Fig. 1c shows the CVs performed at the potential range of 0.0–1.2 V *versus* Ag/AgCl for the MMO and 0.0–2.5 V *versus* Ag/AgCl for the BDD at a scan rate of 50 mV s^{-1} in the urine matrix. Both anodes display different behavior. The MMO has a typical profile of active anodes with a large double-layer region in the potential range preceding the oxygen evolution reaction [27], while BDD presents a typical behavior of non-active anodes with a high O_2 overpotential and low background currents [22].
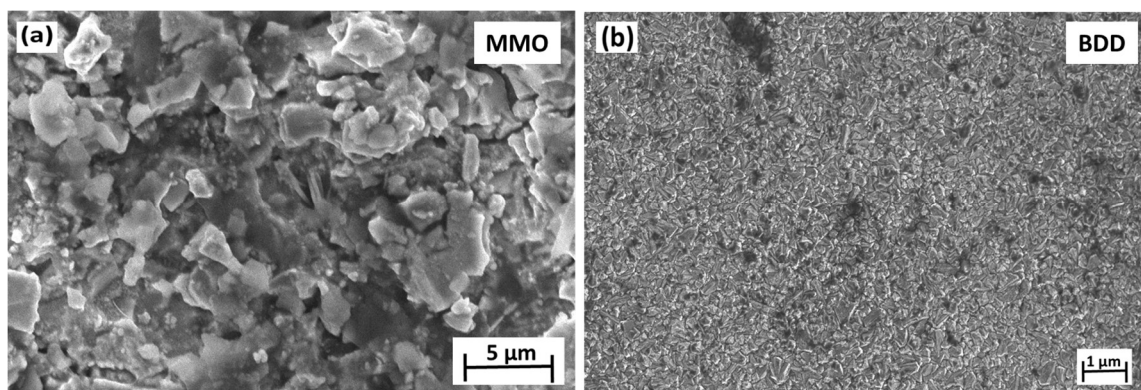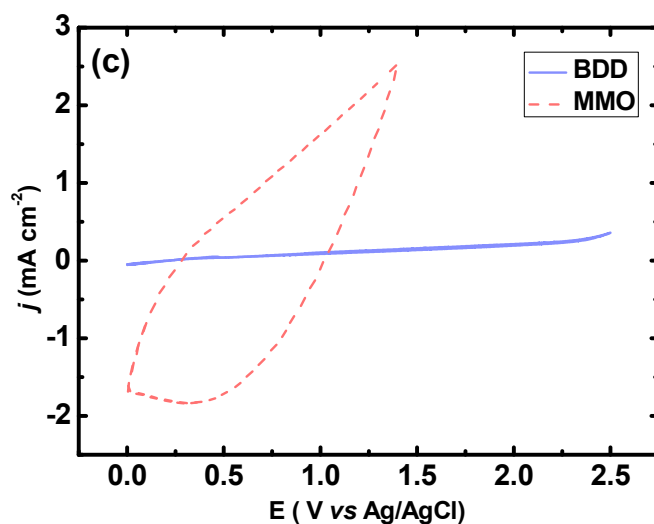
Fig. 1. SEM images of anodes (a) MMO-Ti/RuO$_2$IrO$_2$ and (b) BDD; (c) Cyclic voltammetry curves obtained at 50 mV s^{-1} for both studies anodes.

Fig. 2 shows the removal of Penicillin G during the electrolysis and photo-electrolysis of synthetic urine solutions containing 50 mg dm^{-3} of the Penicillin G (Pen G) using MMO-Ti/RuO$_2$IrO$_2$ and BDD as electrodes. Results are compared with removal attained by single photolysis.

After 8 hours of treatment, around 30% of Pen G contained in the synthetic urine is degraded by photolysis, while electrochemical-based techniques seem to be much more effective, regardless of the anode used. The complete depletion of raw antibiotics in the fixed reaction time (8 h) is just reached by the photo-electrolysis. In the first stages of electrochemical processes with both anodes, rapid degradation of Pen G is observed, and after passing an electric charge of 1.6 Ah L^{-1}, the concentration of Pen G decreased from 50 to 6–12 mg L^{-1}. From this point, the removal becomes slower, and this indicates that electric current supplied is mainly used in side-reactions (regarding the removal of the antibiotic): the oxidation of other compounds contained in the urine.
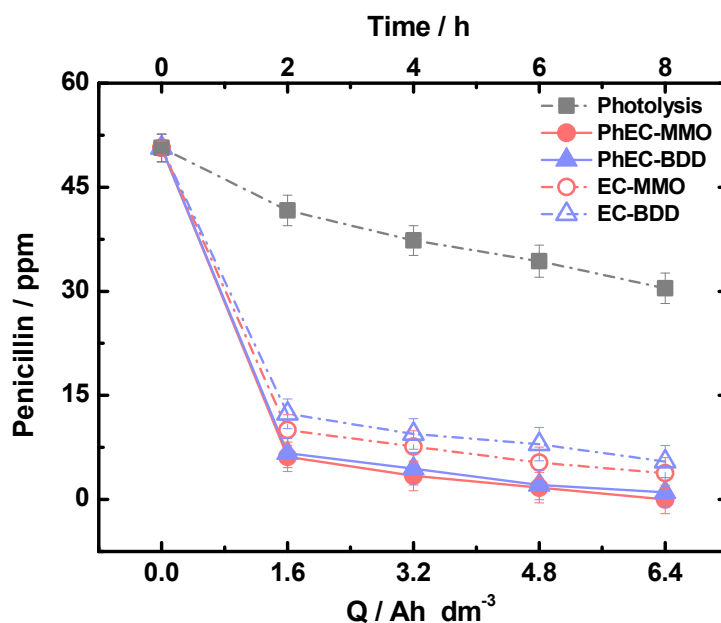
Fig. 2. Degradation of Penicillin G during photolysis (■), electrolysis (empty symbols), and photo-electrolysis (full symbols) of synthetic urine solutions using BDD (▲, △) and MMO-Ti/RuO$_2$IrO$_2$ (●, ○) anodes. Current density applied in electrochemical processes: 30 mA cm^{-2}. UV-light power applied in irradiated processes: 9 W. The error bars represent the standard deviations from duplicate tests.

Since urine medium is exceptionally complex, besides Pen G, other organic compounds (including urea, creatinine, and uric acid) are contained in similar, or even higher, concentrations than Pen G. They can also be oxidized, and their oxidation competes with drug degradation [8]. Fig. 3 shows the removal of these organics naturally contained in human urine with the three studied technologies.

Photolysis is relatively inefficient for removing all organic urine compounds, being even less efficient in the removal of Pen G. Conversely, electrochemical processes can remove them, although the reactivity of each organic compound is different. Uric acid removal shows a similar removal trend to Pen G: rapid oxidation during the first stages of the treatment and complete removal after 8 h of treatment. On the contrary, an electrical

charge of 6.4 Ah dm^{-3} is not enough to degrade urea and creatinine completely, and around 2000 and 60 mg dm^{-3} of each compound, respectively, remain in the urine after electrolysis treatments. As in the case of Pen G, photo-electrolysis shows better performance. So, uric acid is completely removed, around 82% of initial creatinine is degraded, and between 55–70 % of urea is degraded using BDD and MMO-Ti/RuO$_2$IrO$_2$ anode, respectively. These results confirm that antibiotics and uric acid are oxidized more easily than urea and creatinine. It opens the possibility of developing selective oxidation processes, with a great economic impact on the reduction of the hazardousness of effluents contained high concentrations of antibiotics, such as hospital effluents.
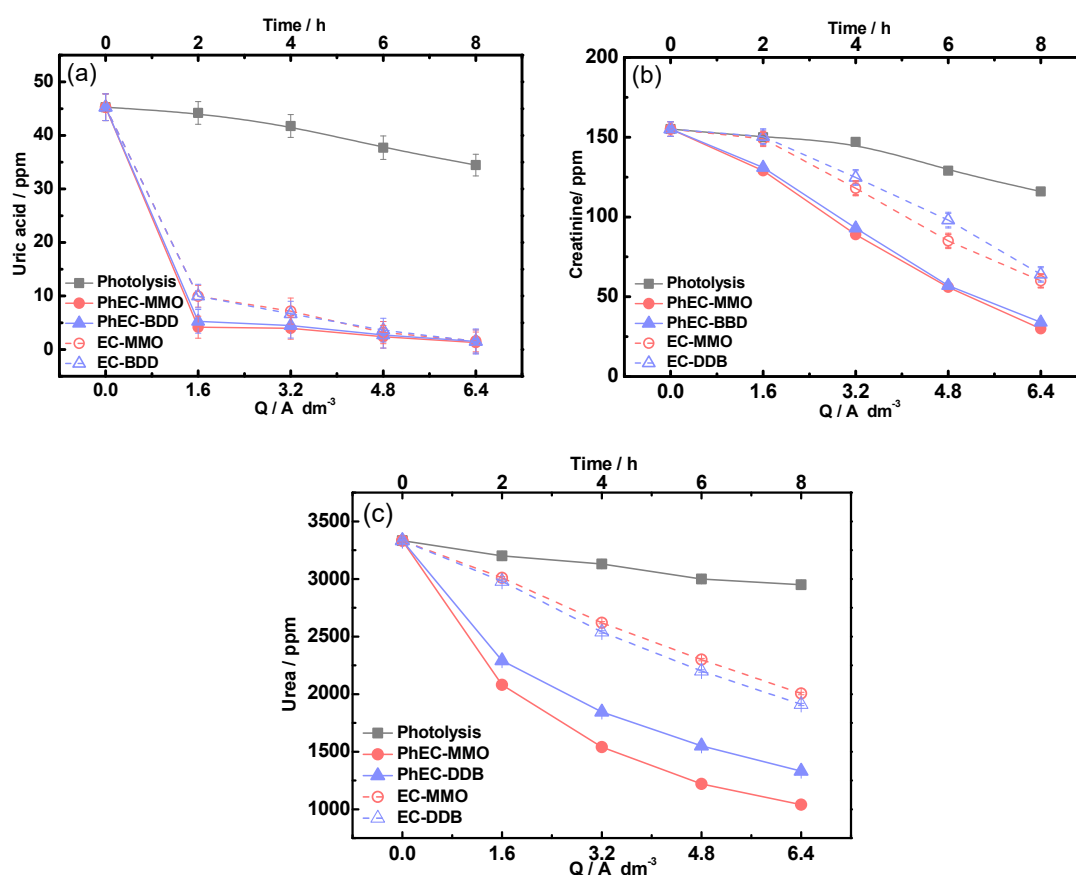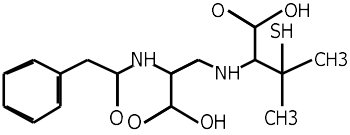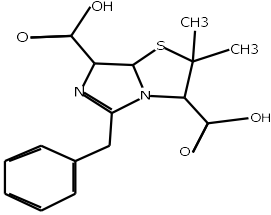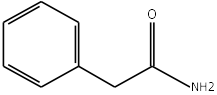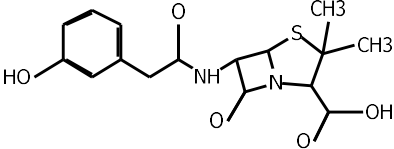

Fig. 3. Degradation of uric acid (a), creatinine (b), and urea (c) during photolysis (■), electrolysis (empty symbols), and photo-electrolysis (full symbols) of synthetic urine solutions using BDD (▲,△) and MMO-Ti/RuO$_2$IrO$_2$ (●, ○) anodes. Current density applied

in electrochemical processes: 30 mA cm^{-2}. UV-light power applied in irradiated processes: 9 W. The error bars represent the standard deviations from duplicate tests.

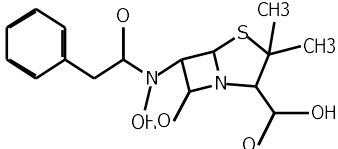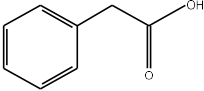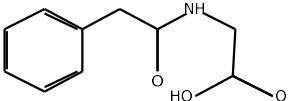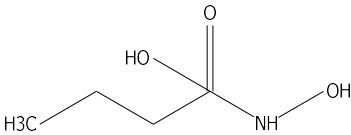Removal of a given compound does not always mean mineralization but merely its transformation into other species, as shown in Fig. SM1, where the trends of the leading high molecular weight intermediates detected during the electrolysis photoelectrolysis with BDD and MMO are plotted. These intermediates have been identified by HPLC-MS, and they are according to those previously reported in the literature [28–34]. Table 2 summarizes the treatment in which they are formed, their formula, chemical structure, and mass-to-charge (m/z).

Table 2. Primary high molecular weight intermediates detected during electrolysis and photo-electrolysis with BDD and MMO.

Process	Formula	Feasible structure	m/z	According to reference
EC-BDD	$C_{16}H_{20}N_2O_5S$		352.1092	[28, 29]
EC-BDD EC-MMO	$C_{16}H_{18}N_2O_4S$		334.0987	[30, 31]
PhEC-BDD PhEC-MMO	C_8H_9NO		135.0684	[32]

EC-BDD EC-MMO PhEC-BDD PhEC-MMO	$C_{16}H_{18}N_2O_5S$		353.1171	[32]
EC-BDD EC-MMO PhEC-BDD PhEC-MMO	$C_{16}H_{18}N_2O_5S$		353.1171	[32]
EC-BDD EC-MMO PhEC-BDD PhEC-MMO	$C_8H_8O_2$		136.0524	[33]
PhEC-BDD	$C_{10}H_{11}NO_3$		193.0738	[34]
EC-BDD PhEC-BDD PhEC-MMO	$C_4H_{10}NO_3$		120.0660	–

The chemical oxygen demand (COD) and the total organic carbon (TOC) have also been monitored to inform about global oxidation and global mineralization progress. Fig. 4 shows the removal achieved after 1.6 and 6.4 A h dm^3 charges, applied to treatments with photolysis and electrochemical-based technologies with MMO- Ti/RuO$_2$IrO$_2$ and BDD anodes at 30 mA cm^{-2}. Note that photolysis is inefficient in removing TOC, but it attains around 39% of COD removal, meaning that this technology transforms compounds but cannot mineralize them. Meanwhile, electrolysis and photo-electrolysis remove around 50%

TOC and 75–80% of COD regardless of the anode used again. Photo-electrolysis using MMO-Ti/RuO$_2$IrO$_2$ anode stands out, with reductions of 55% and 76% for TOC and COD, respectively.
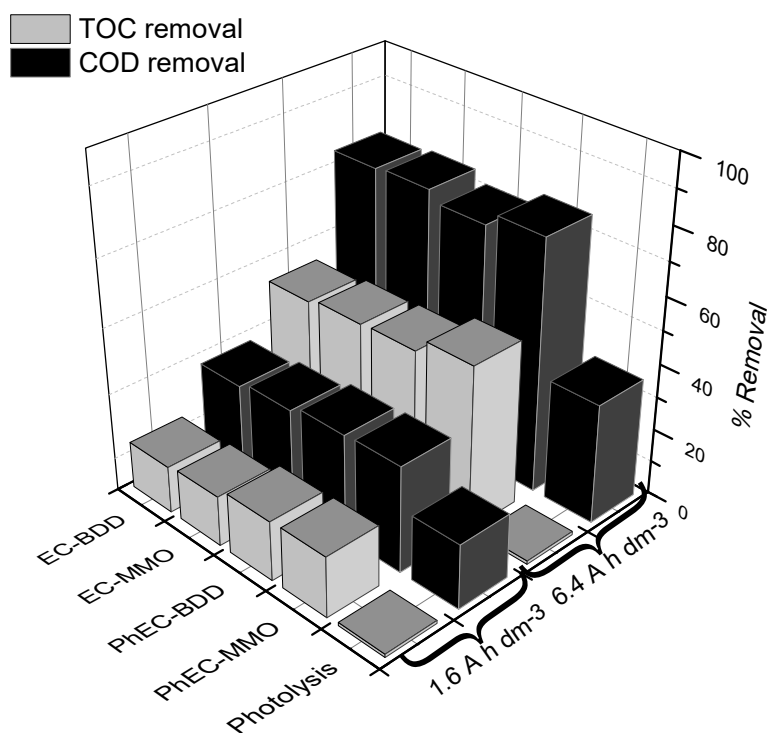
Fig. 4. COD (black bars) and TOC (white bars) removal on the different processes with MMO-Ti/RuO$_2$IrO$_2$ and BDD anodes in Penicillin G in charges (a) 1.6 A h dm^3 (b) 6.4 A h dm^3. Conditions: current density 30 mA cm^{-2}, TOC$_{initial}$: 798 mg L^{-1} e COD$_{initial}$: 398 mg L^{-1}.

Again, these results indicate the good performance of MMO-Ti/RuO$_2$IrO$_2$ anodes in terms of total degradation (COD removal) and complete oxidation to carbon dioxide (TOC removal). Besides, it opens the opportunity to use MMO electrolysis to remove antibiotics from a complex matrix (as urine) with high efficiency, minimizing the losses of energy in side processes. TOC and Pen G removals are plotted in semi-log (Fig. 5) to point out this

remark. As seen, they follow a linear trend, indicating that electrolysis, photolysis, and photo-electrolysis of synthetic urines fit well to first-order kinetics (Eq. 3) [17]. However, for Penicillin G removal, it is possible to observe not only one but two regions of first-order kinetics for electrolysis and three regions for photo-electrolysis. These outcomes suggest a change in the oxidation mechanism of organic matter during the electrolysis and photo-electrolysis tests [27].
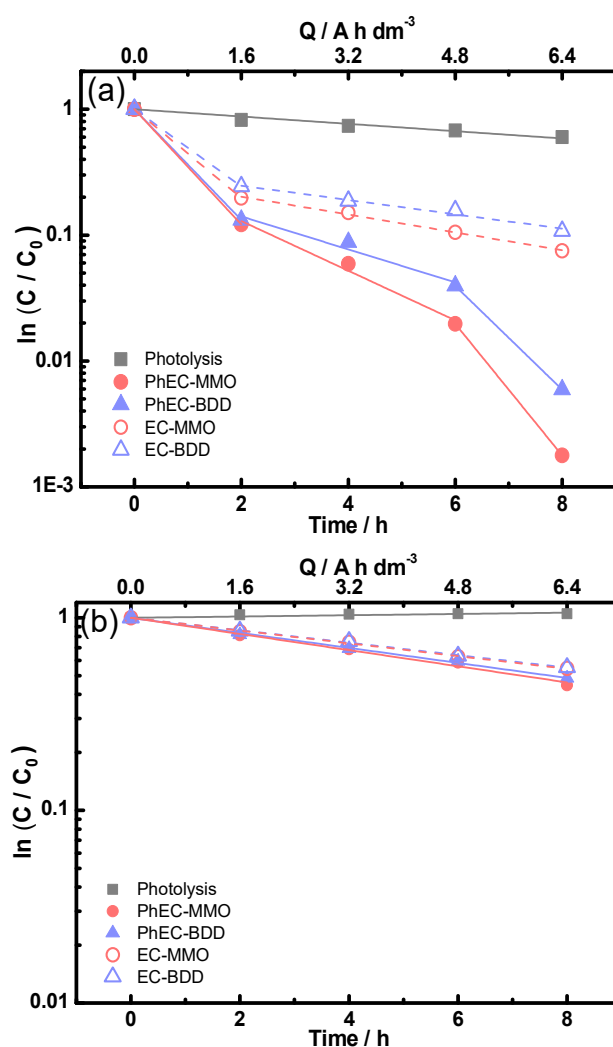
$$ln\frac{c_0}{c} = k.t \tag{3}$$

Fig. 5. Kinetics of the removal for electrolysis, photolysis, and photo-electrolysis using MMO-Ti/RuO$_2$IrO$_2$ or BDD of (a) Pen G and (b) TOC

The first transition of kinetic observed in electrochemically-based technologies occurs when approximately 75–85% of Pen G is converted into organic intermediates, and low molecular weight carboxylic acids [27,35] is expected. They generally have very different oxidation behavior regarding the raw antibiotic, which helps explain the observed change. Concerning the second transition of the kinetic observed in photo-electrolysis tests, the initial slope is recovered (parallel to stage 1), suggesting that this competition disappeared due to the depletion of the competing intermediates formed. For TOC removal, only one first-order kinetic region is observed for all cases.
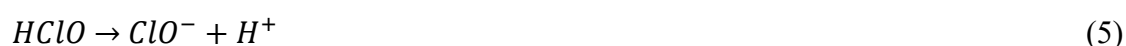
The rate constants for the Pen G removal and mineralization of the different processes are summarized in Table 3. In general, the k_{PenG} values are higher than K_{TOC}. In the case of photolysis K_{TOC} is zero (no mineralization), and K_{PenG} is one-log lower than in electrochemical-based technologies due to the nil mineralization and the lower Pen G degradation. Both kinetic constants are lower in the electrolysis than in photo-electrolysis, being these differences higher in terms of Pen G removal. It indicates that the irradiation with UV light during electrochemical oxidation promotes the selectivity towards Pen G degradation but not the mineralization. The effect of anode used has low relevance, although MMO shows a higher percentage of removal and, hence, higher kinetic constant values.

Table 3. Kinetic constants and synergistic coefficient of the combined photo-electrolysis process using MMO and BDD electrodes.

Process	Constants kinetics				Synergistic coefficient (%)			
	Penicillin G			*TOC*	*Penicillin G*			*TOC*
	k_1	k_2	k_3	k_1	Zone 1	Zone 2	Zone 3	–
PhEC-MMO	0.46	0.19	0.52	0.04	21	100	420	11
PhEC-BDD	0.44	0.13	0.41	0.04	33	40	355	14

EC-MMO	0.35	0.06	–	0.03		–	–
EC-BDD	0.30	0.07	–	0.03		–	–
Photolysis	0.03	–	–	0.003	–	–	–	–

Another essential parameter that informs about the relevance of combining technologies is the synergistic coefficient because it quantifies if the combination of removal technologies is synergistic, merely additive, or even antagonistic. Table 2 also shows the synergistic coefficient for three-zone estimated for Pen G degradation and one-zone for mineralization. For Pen G, the synergistic coefficient increases (420%) with photo-electrolysis time and reaches its maximum when MMO-Ti/RuO$_2$IrO$_2$ is used. This coefficient is relevant but small compared to the photo-electrolysis of wastewater polluted with other pharmaceutical products and pesticides [8,21], which can reach up to 700–900%. However, small coefficient values are found for TOC, with a maximum of 11–14%. Once again, it indicates that UV-radiation during electrochemical oxidation seems to promote selectivity in relation to Pen G degradation since the synergistic effect regarding TOC is irrelevant. This synergic effect can be explained in terms of different mechanisms involving the formation of reactive chlorine species, which are initially present in the urine matrix (1000 mg dm^{-3} of chlorine). Chlorine can be generated on the anode surface (Eq. 3) [42,43], and it can be transformed in bulk into hypochlorous acid/hypochlorite (Eqs. 4–5) [37].

$$Cl^- \rightarrow Cl_2 + 2e^- \qquad (3)$$

$$Cl_2 + 2H_2O \rightarrow HClO + Cl^- + H^+ \qquad (4)$$

$$HClO \rightarrow ClO^- + H^+ \qquad (5)$$

When BDD anodes are used, large quantities of hydroxyl radicals are formed, coexisting with chlorine species [38]. Additionally, these hydroxyl radicals can oxidize Cl$^-$

to different oxochlorinated compounds by Eqs. (6–10) [21], which leads to the formation of non-useful and hazardous chlorate and perchlorate.

$$H_2O \rightarrow BDD\,^{\circ}OH + H^+ + e^- \tag{6}$$

$$Cl^- + \,^{\circ}OH \rightarrow ClO^- + H^+ + e^- \tag{7}$$

$$ClO^- + \,^{\circ}OH \rightarrow ClO_2^- + H^+ + e^- \tag{8}$$

$$ClO_2^- + \,^{\circ}OH \rightarrow ClO_3^- + H^+ + e^- \tag{9}$$

$$ClO_3^- + \,^{\circ}OH \rightarrow ClO_4^- + H^+ + e^- \tag{10}$$

The synergism between the MMO-Ti/RuO$_2$IrO$_2$ anode and the UVC light results in the homolysis reaction of HClO to produce hydroxyl and chlorine radicals that are responsible for the Pen G degradation in the bulk solution [20]. In the case of BDD, the slightest synergistic effect is likely due to the low amounts of electrogenerated HClO species and their parasitic oxidation reactions to produce ClO_3^- (Eq. 9) and ClO_4^- (Eq. 10), mediated by hydroxyl radicals produced on the surface of BDD by H$_2$O oxidation [39].

Note that although the removal of Penicillin G and/or organic load is attained, no information is provided on the riskiness of the treated effluent that contains not only the raw antibiotic in lower concentration but also its degradation products. Thus, it must be clarified if the riskiness of urine is related to the toxicity of organic and inorganic species contained or to the antibiotic resistance that antibiotics can cause when the bacteria mutate in response to their accumulation in the environment. To do this, widely used toxicity tests based on the use of the bioluminescent marine bacterium *Vibrio Fisheri* and the most recent method developed to quantify antibiotic resistance using *Enterococcus faecalis* as the target bacterium [35] were carried out. The information obtained with these microbiological methods, together with the physicochemical characterization, will help to establish the ideal

operating conditions and the reaction time to reduce the chemical risk of hospital urine wastes.

The aliquots removed after the application of 1.6 A h dm^{-3} were analyzed to evaluate these parameters since, at this point, Penicillin G was almost completely removed (see Fig. 2). Fig 6 shows the inhibition percentage (estimated by toxicity test) of the treated urine by electrolysis and photo-electrolysis at 30 mA cm^{-2} using both anodes. Initially, around 95% of inhibition was obtained, clearly indicating that synthetic urine polluted with 50 mg dm^{-3} of Pen G inhibits the activity of *Vibrio fischeri*. After passing 1.6 A h dm^{-3}, the bacterial inhibition decreases below 15%, and, again, the vital influence of both the anode material and the irradiation with UV light are demonstrated.
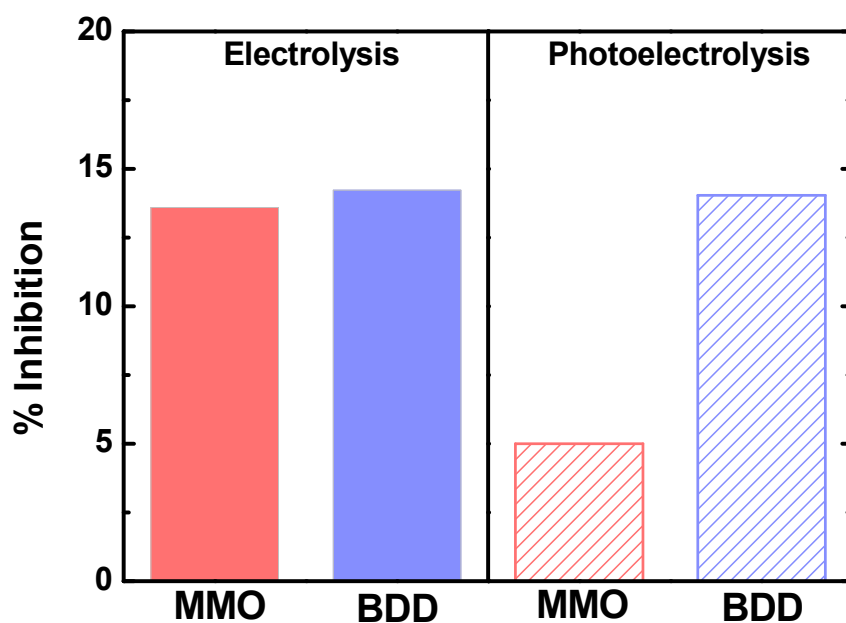

Fig. 6. Effect of electrolysis and photo-electrolysis on the toxicity of treated solutions employing MMO and BDD anodes using the bioluminescent bacteria *Vibrio fischeri*. Conditions: Pen G (50 mg dm^{-3}) in synthetic urine using a charge of 1.6 Ah dm^{-3}.

The photo-electrolysis with MMO-Ti/RuO$_2$IrO$_2$ shows the lowest inhibition (around 5%) that can be related to the nature of organic and inorganic species accumulated in the reaction medium. These species come from the partial degradation of Pen G (and/or other urine-organics), as well as from the oxidation of inorganic species contained in urine such as chloride, sulfate, phosphate, or carbonates. With MMO anodes, chloride can be oxidized electrochemically and favors hypochlorite formation [40], but the formation of chlorate or perchlorate is not expected. On the contrary, when using BDD anodes, the formation of highly-oxidized chloro species and peroxosulphate, peroxophosphate, or peroxocarbonate is expected; this could explain the inferior results obtained in terms of toxicity [41]. Nevertheless, their contribution was excluded by the addition of sodium sulfite (with a ratio of mol sodium sulfate/mol oxidants quantified by I$^-$/I$_2$ titration) before toxicity analysis. Hence, the inhibition measures are only associated with the organics contained and not with toxic inorganic species.

However, this method only informs about the response of a given bacterium (*Vibrio fischeri*) to compounds contained in the urine matrix. Therefore, to complete this information and evaluate the risk of accumulating antibiotics in the environment, the antibiotic resistance was evaluated by exposure to a gram-positive bacteria, *Enterococcus faecalis* [42]. *Enterococci* are intrinsically resistant to many commonly used antimicrobial agents, but they exhibit decreased penicillin susceptibility. Thus, it could be a good indicator of the antibiotic effect of treated urine. Fig. 7 shows the results obtained in these antibiotic-resistance tests, in which each sample was measured by quadruplicate. In case of urine still containing antibiotic effect, the decrease of CFU should be observed, indicating the potential ecotoxicity risk of each urine sample. The antibiotic effect of the treated urine is still high after electrolysis due to the presence of Penicillin (or its metabolites) that still cause the deactivation of the bacterium (from 10^7 to 10^3 CFU mL^{-1}). Conversely, the population of *E.*

faecalis decreases insignificantly when it is merged with urine treated by photo-electrolysis with MMO anode (*E. faecalis* population remains around 10^7 CFU mL^{-1}). This outcome is indicative of the low ecotoxicity risk of this sample and, therefore, its release into the environment should not have any relevant adverse effect.
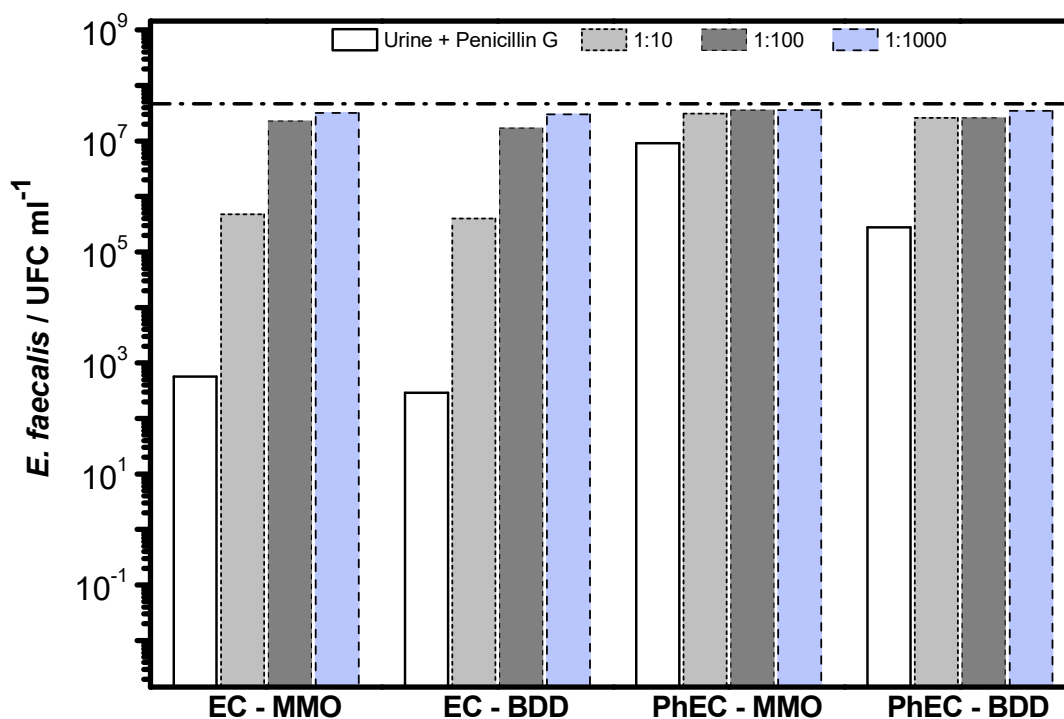

Fig 7. Antibiotic effect of urine treated by different electrochemical-based processes. Electric charge passed: 1.6 Ah dm^{-3}.

These results have been compared with previous reports from the literature in which the degradation of pharmaceuticals using AOPs (photochemical and electrochemical) was evaluated, and the antibiotic effect of treated effluents was also tested. The direct comparison of these results is not an easy task due to the different experimental conditions tested, aqueous matrix, electrodic material used, electrical charge passed, and microbiological technique used. Table 4 summarizes the experimental conditions and the main results reported.

In general, it can be stated the vital role of the aqueous matrix: the degradation process seems to be more efficient in natural and municipal wastewater than in the urine matrix [35, 43]. Perea et al. [35] reported that the electrolysis with Ti/RuIr anode is able to remove the target antibiotic (cephalexin) in less than 2 hours operating at a current density of 4 mA cm^{-2}. However, around 40% of residual antimicrobial activity still remains after this treatment. Similar results are reported by Jojoa-Sierra et al. [43] during the electrolysis of urine solutions containing Norfloxacin: the antibiotic is removed after 3 hours of treatment at 6.53 mA cm^{-2}, but more than 6 hours are required to deplete the antibiotic effect. This delay could be related to the formation of intermediates with antibiotic effects. These results agree with those obtained during electrolysis with MMO and BDD of Pen G in urine media.

Nevertheless, the irradiation of light seems to be a key parameter in antibiotic removal and antibiotic resistance removal (as shown in Fig 1 and 6). This fact has been previously reported for the removal of antibiotics in wastewater [44–46] but not in urine media. Nonetheless, according to results obtained in this work, we can state that the photoelectrolysis is a suitable technology for decreasing the riskiness of hospital urine and operating at 30 mA cm^{-2} (current density) and 9 W (light irradiation) the antibiotic activity of the urine can be removed entirely in less than 2 hours of treatment (and 1.6 Ah dm^{-3} of electrical charged passed). Therefore, the present study results again confirm the outstanding performance of MMO-Ti/RuO$_2$IrO$_2$ to treat hospital wastewater.

Table 4. Comparison of the performance antibiotic resistance removal

Initial Waste	Treatment technology	Results	Reference
Antibiotic: Cephalexin *Matrix:* Urine, distilled water,	*Electrochemical oxidation* $t = 2$ h $j = 4$ mA cm^{-2} $C_0 = 0.86$ mM	*Antibiotic removal*: 100% *Antibiotic resistance removal*: urine 60%, distilled water, and municipal wastewater 100%	Perea et al. [35]

and municipal wastewater	*Anode* = Ti/Ru-Ir	***Antibiotic activity assay***: Staphylococcus aureus / Disk diffusion method	
Antibiotic: Norfloxacin ***Matrix:*** Urine, seawater, and municipal wastewater	***Electrochemical oxidation*** t = 2–6 h j = 6.53 mA cm^{-2} C_0 =125 μM *Anode* = Ti/IrO$_2$	***Antibiotic removal:*** Seawater: 100% in 1 h, municipal wastewater: 100% in 2 h, urine: 70% in 3 h ***Antibiotic resistance removal***: Seawater: 100% in 1 h, municipal wastewater: 100% in 6 h, urine: 100% in more 6 h ***Antibiotic activity assay***: Staphylococcus aureus / Agar diffusion test	Jojoa-Sierra et al. [43]
Antibiotic: Cloxacillin ***Matrix:*** natural mineral water and Glucose	***Electrochemial, photocatalysis and photoFenton*** t = 2.5 h j = 30 mA cm^{-2} C_0 =203 μM *Anode* = Ti/IrO$_2$	***Antibiotic removal:*** 100% ***Antibiotic resistance removal***: 100% ***Antibiotic activity assay***: Staphylococcus aureus / Disk diffusion method	Serna-Galvis et al. [44]
Antibiotic: Oxacillin ***Matrix:*** NaCl 0.22M, Natural water and Glucose	***Electrochemical oxidation*** t = 1 h j = 30.25 mA cm^{-2} C_0 = 203 μM *Anode* = Ti/IrO$_2$	***Antibiotic removal:*** 100% ***Antibiotic resistance removal***: 100% ***Microbiological technique used***: Staphylococcus aureus / Disk diffusion method	Giraldo et al. [47]
Antibiotic: Ciprofloxacin ***Matrix***: NaCl 0.5M	***Electrochemical oxidation*** t = 60 min j = 17 mA cm^{-2} / C_0 = 15 mM *Anode* = Ti/RuO$_2$ or Ti/SbRuZr	***Antibiotic removal:*** 100% ***Antibiotic resistance removal***: 100% ***Antibiotic activity assay***: Staphylococcus aureus / Disk diffusion method	Palma Goyes et al. [36]
Antibiotic: Chloramphenicol ***Matrix***: distilled water	***UV/H$_2$O$_2$*** t = 50 min Lamp= 6 W and 254 nm [H$_2$O$_2$] = 35mM C_0 = 150 mg L^{-1}	***Antibiotic removal:*** 100% ***Antibiotic resistance removal***: 100% ***Antibiotic activity assay***: Staphylococcus aureus / Agar-well diffusion method	Zuorro et al. [45]
Antibiotics: Ciprofloxacin ***Matrix***: Distilled water and natural water	***Fe^{2+}/H$_2$O$_2$/UV$_{365}$ H$_2$O$_2$/UV$_{254}$ TiO$_2$/UV$_{365}$*** Lamp=30 W [H$_2$O$_2$] = 4.2 mM [Fe^{2+}] = 0.09 mM [TiO$_2$] = 0.05 g L^{-1} C_0= 0.052 mM	***Antibiotic removal:*** 100% Fe^{2+}/H$_2$O$_2$/UV$_{365}$ in 120 min, 100% H$_2$O$_2$/UV$_{254}$ in 480 min and 100% TiO$_2$/UV$_{365}$ in 480 min ***Antibiotic resistance removal***: 100% ***Antibiotic activity assay***: Staphylococcus aureus / Disk diffusion method	Villegas-Guzman et al. [46]

Antibiotics: Ofloxacin and Ciprofloxacin *Matrix:* Water and meat effluent	*Atmospheric cold plasma* Voltage=70–80 kV t= 5–25 min T < 5°C $C_0 = 10$ mg L^{-1} v = 25 mL	**Antibiotic removal:** 90 and 95% *Antibiotic resistance removal:* ~90% *Antibiotic activity assay:* *Staphylococcus aureus* / Disk diffusion assay and Broth microdilution method	Sarangapani et al. [48]
Antibiotic: Penicillin G *Matrix:* Urine	*Photo-electrochemical* t = 8 h $j = 30$ mA cm^{-2} $C_0 = 50$ mg L^{-1} *Anode* = MMO-Ti/RuO$_2$IrO$_2$ or BDD	**Antibiotic removal:** 100% *Antibiotic resistance removal:* ~100% *Microbiological technique used:* *Enterococus Faecalis* / Impedance detection	This work

The obtained results also point out the relevance of using different characterization techniques to quantify toxicity, because each of them gives very different and complementary information. On the other hand, the quantification of the specific energy consumption (SEC) is also of great relevance to evaluate the possible application of an electrochemical-based technology from an economic point of view, due to it globalizes the main operating cost of each technology, that is, the electric current applied in electrochemical processes and the energy consumed by the UV-lamp. Fig. 8 shows the SEC when the charge applied was 1.6 and 6.4 A h dm^{-3} for both electrochemically based technologies tested in this work. As seen, the SEC increases for PhEC-BDD, which indicates that the integration of technologies is not showing a clear advantage from the energy point of view. On the contrary, the higher reactivity of the MMO-Ti/RuO$_2$IrO$_2$ with the chlorides contained in the urine may explain the lower energy consumption observed and confirms the excellent perspective of MMO-Ti/RuO$_2$IrO$_2$ electrodes.
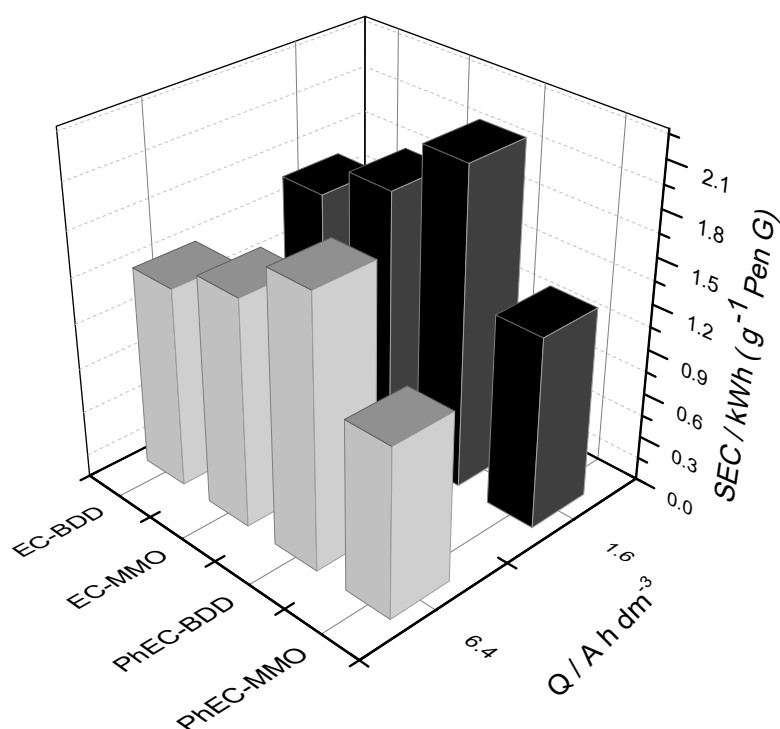
Fig. 8. Specific energy consumption for the electrochemical (EC) and photo-electrochemical (PhEC) processes carried out at 30 mA cm^{-2} in urine by using MMO-Ti/RuO$_2$IrO$_2$ and BDD anodes.

4. Conclusions

According to the results obtained from this study, the following conclusions are drawn:

- Penicillin G can be degraded efficiently using electrolysis and photo-electrolysis with MMO-Ti/RuO$_2$IrO$_2$ and BDD anodes. Synergism of electrolytic and photolytic treatments is important and reached a value of 420% for photo-electrolysis with MMO-Ti/RuO$_2$IrO$_2$.

- The most efficient technique for degrading the main organic components contained in urine (urea, creatinine, and uric acid) is photo-electrolysis using MMO-Ti/RuO$_2$IrO$_2$ anode. This technology obtained the maximum removal of TOC and COD that was 55 and 76%, respectively, in 8 hours of treatment.

- In the toxicity tests, it is observed that the anode used in the electrolysis does not influence the final toxicity of the solution. However, only MMO-Ti/RuO$_2$IrO$_2$ can generate solutions with almost zero residual toxicity when photo-electrolysis is used.

- Similar to toxicity, after photo-electrolysis with MMO-Ti/RuO$_2$IrO$_2$ anode, there is no antibiotic effect in the treated urine.

5. References

[1] C. Comninellis, Electrocatalysis in the Electrochemical Conversion / Combustion of Organic Pollutants, Electrochim. Acta. 39 (1994) 1857–1862. doi:10.1016/0013-4686(94)85175-1.

[2] M.M. Petrović, J.Z. Mitrović, M.D. Antonijević, B. Matović, D. V. Bojić, A.L. Bojić, Synthesis and characterization of new Ti-Bi$_2$O$_3$ anode and its use for reactive dye degradation, Mater. Chem. Phys. 158 (2015) 31–37. doi:10.1016/j.matchemphys.2015.03.030.

[3] M. Zhou, H. Särkkä, M. Sillanpää, A comparative experimental study on methyl orange degradation by electrochemical oxidation on BDD and MMO electrodes, Sep. Purif. Technol. 78 (2011) 290–297. doi:10.1016/j.seppur.2011.02.013.

[4] F.L. Migliorini, N. a. Braga, S. a. Alves, M.R. V Lanza, M.R. Baldan, N.G. Ferreira, Anodic oxidation of wastewater containing the Reactive Orange 16 Dye using heavily boron-doped diamond electrodes, J. Hazard. Mater. 192 (2011) 1683–1689. doi:10.1016/j.jhazmat.2011.07.007.

[5] S. Dbira, N. Bensalah, P. Cañizares, M.A. Rodrigo, A. Bedoui, The electrolytic treatment of synthetic urine using DSA electrodes, J. Electroanal. Chem. 744 (2015) 62–68. doi:10.1016/j.jelechem.2015.02.026.

[6] F.C. Moreira, S. Garcia-Segura, R.A.R. Boaventura, E. Brillas, V.J.P. Vilar, Degradation of the antibiotic trimethoprim by electrochemical advanced oxidation processes using a carbon-PTFE air-diffusion cathode and a boron-doped diamond or platinum anode, Appl. Catal. B Environ. 160–161 (2014) 492–505. doi:10.1016/j.apcatb.2014.05.052.

[7] S. Dbira, N. Bensalah, M.I. Ahmad, A. Bedoui, Electrochemical oxidation/disinfection of urine wastewaters with different anode materials, Materials (Basel). 12 (2019) 1254. doi:10.3390/ma12081254.

[8] S. Cotillas, E. Lacasa, C. Sáez, P. Cañizares, M.A. Rodrigo, Disinfection of urine by conductive-diamond electrochemical oxidation, Appl. Catal. B Environ. 229 (2018) 63–70. doi:10.1016/j.apcatb.2018.02.013.

[9] W. Wu, Z.H. Huang, T.T. Lim, Recent development of mixed metal oxide anodes for electrochemical oxidation of organic pollutants in water, Appl. Catal. A Gen. 480 (2014) 58–78. doi:10.1016/j.apcata.2014.04.035.

[10] S. Trasatti, Electrocatalysis: understanding the success of DSA®, Electrochim. Acta. 45 (2000) 2377–2385. doi:10.1016/S0013-4686(00)00338-8.

[11] M. Wang, Z. Wang, X. Gong, Z. Guo, The intensification technologies to water electrolysis for hydrogen production – A review, Renew. Sustain. Energy Rev. 29 (2014) 573–588. doi:10.1016/j.rser.2013.08.090.

[12] J. Li, Z. Yang, H. Xu, P. Song, J. Huang, R. Xu, Y. Zhang, Y. Zhou, Electrochemical treatment of mature landfill leachate using Ti/RuO_2–IrO_2 and Al electrode: optimization and mechanism, RSC Adv. 6 (2016) 47509–47519. doi:10.1039/C6RA05080H.

[13] T.É.S. Santos, R.S. Silva, K.I.B. Eguiluz, G.R. Salazar-Banda, Development of $Ti/(RuO_2)_{0.8}(MO_2)_{0.2}$ (M=Ce, Sn or Ir) anodes for atrazine electro-oxidation. Influence of the synthesis method, Mater. Lett. 146 (2015) 4–8. doi:10.1016/j.matlet.2015.01.145.

[14] T. Audichon, S. Morisset, T.W. Napporn, K.B. Kokoh, C. Comminges, C. Morais, Effect of Adding CeO_2 to RuO_2-IrO_2 Mixed Nanocatalysts: Activity towards the Oxygen Evolution Reaction and Stability in Acidic Media, ChemElectroChem. 2 (2015) 1128–1137. doi:10.1002/celc.201500072.

[15] T. Audichon, T.W. Napporn, C. Canaff, C. Morais, C. Comminges, K.B. Kokoh, IrO_2 coated on RuO_2 as efficient and stable electroactive nanocatalysts for electrochemical water splitting, J. Phys. Chem. C. 120 (2016) 2562–2573. doi:10.1021/acs.jpcc.5b11868.

[16] I.M.D. Gonzaga, A.R. Dória, V.M. Vasconcelos, F.M. Souza, M.C. dos Santos, P. Hammer, M.A. Rodrigo, K.I.B. Eguiluz, G.R. Salazar-Banda, Microwave synthesis of $Ti/(RuO_2)_{0.5}(IrO_2)_{0.5}$ anodes: Improved electrochemical properties and stability, J. Electroanal. Chem. 874 (2020) 114460. doi:10.1016/j.jelechem.2020.114460.

[17] A.N. Subba Rao, V.T. Venkatarangaiah, Metal oxide-coated anodes in wastewater treatment, Environ. Sci. Pollut. Res. 21 (2014) 3197–3217. doi:10.1007/s11356-013-2313-6.

[18] M.J. Martín de Vidales, M. Millán, C. Sáez, P. Canizares, M.A. Rodrigo, Irradiated-assisted electrochemical processes for the removal of persistent pollutants from real wastewater, Sep. Purif. Technol. 175 (2017) 428–434. doi:10.1016/j.seppur.2016.11.014.

[19] F.L. Souza, C. Saéz, M.R.V. Lanza, P. Cañizares, M.A. Rodrigo, Removal of herbicide 2,4-D using conductive-diamond sono-electrochemical oxidation, Sep. Purif. Technol. 149 (2015) 24–30. doi:10.1016/j.seppur.2015.05.018.

[20] I. Sánchez-Montes, J.F. Pérez, C. Sáez, M.A. Rodrigo, P. Cañizares, J.M. Aquino, Assessing the performance of electrochemical oxidation using DSA$^{®}$ and BDD anodes in the presence of UVC light, Chemosphere. 238 (2020). doi:10.1016/j.chemosphere.2019.124575.

[21] G.O.S. Santos, K.I.B. Eguiluz, G.R. Salazar-Banda, C. Saez, M.A. Rodrigo, Photo-electrolysis of clopyralid wastes with a novel laser-prepared MMO-RuO_2TiO_2 anode, Chemosphere. 244 (2020) 125455. doi:10.1016/j.chemosphere.2019.125455.

[22] H. Rubí-juárez, S. Cotillas, C. Sáez, P. Cañizares, C. Barrera-Díaz, M.A. Rodrigo, Use of conductive diamond photo-electrochemical oxidation for the removal of pesticide glyphosate, 167 (2016) 127–135. doi:10.1016/j.seppur.2016.04.048.

[23] G.O.S. Santos, L.R.A. Silva, Y.G.S. Alves, R.S. Silva, K.I.B. Eguiluz, G.R. Salazar-Banda, Enhanced stability and electrocatalytic properties of Ti/$Ru_xIr_{1-x}O_2$ anodes produced by a new laser process, Chem. Eng. J. 355 (2019) 439–447. doi:10.1016/j.cej.2018.08.145.

[24] I.M.D. Gonzaga, A.C.A. Andrade, R.S. Silva, G.R. Salazar-Banda, E.B. Cavalcanti, K.I.B. Eguiluz, Synthesis of high-area chemically modified electrodes using microwave heating, Chem. Eng. Commun. 206 (2019) 647–653. doi:10.1080/00986445.2018.1516645.

[25] S. Cotillas, M.J.M. De Vidales, J. Llanos, C. Sáez, P. Ca, M.A. Rodrigo, Electrolytic and electro-irradiated processes with diamond anodes for the oxidation of persistent pollutants and disinfection of urban treated wastewater, J. Hazard. Mater. 319 (2016) 93–101. doi:10.1016/j.jhazmat.2016.01.050.

[26] G.O. Santos, I.M.D. Gonzaga, K.I.B. Eguiluz, G.R. Salazar-Banda, C. Saez, M.A. Rodrigo, Improving biodegradability of clopyralid wastes by photo-electrolysis: The role of anode material, J. Electroanal. Chem. (2020) 114084. doi:10.1016/j.jelechem.2020.114084.

[27] D. Dionisio, A.J. Motheo, C. Sáez, M.A. Rodrigo, Effect of the electrolyte on the electrolysis and photo-electrolysis of synthetic methyl paraben polluted wastewater, Sep. Purif. Technol. 208 (2019) 201–207. doi:10.1016/j.seppur.2018.03.009.

[28] A. Karlesa, G.A.D. De Vera, M.C. Dodd, J. Park, M.P.B. Espino, Y. Lee, Ferrate(VI) Oxidation of β-Lactam Antibiotics: Reaction Kinetics, Antibacterial Activity Changes, and Transformation Products, Environmental Science & Technology 48(17) (2014) 10380–10389. https://doi.org/10.1021/es5028426.

[29] D. Li, M. Yang, J. Hu, Y. Zhang, H. Chang, F. Jin, Determination of penicillin G and its degradation products in a penicillin production wastewater treatment plant and the receiving river, Water Research 42(1) (2008) 307–317. https://doi.org/https://doi.org/10.1016/j.watres.2007.07.016.

[30] J. Chen, P. Sun, X. Zhou, Y. Zhang, C.-H. Huang, Cu(II)–Catalyzed Transformation of Benzylpenicillin Revisited: The Overlooked Oxidation, Environmental Science & Technology 49(7) (2015) 4218–4225. https://doi.org/10.1021/es505114u.

[31] F. Aldeek, W. Hammack, M. Crosswhite, M. Standland, D. Canzani, G. Gerard, J. Cook, LC-MS/MS Validation of a Residue Analysis Method for Penicillin G and Its Metabolites in Commercial Orange Juice, Journal of AOAC International 100 (2016). https://doi.org/10.5740/jaoacint.16-0166.

[32] X. Zhou, D. Liu, Y. Zhang, J. Chen, H. Chu, Y. Qian, Degradation mechanism and kinetic modeling for UV/peroxydisulfate treatment of penicillin antibiotics, Chemical Engineering Journal 341 (2018) 93–101. https://doi.org/https://doi.org/10.1016/j.cej.2018.01.137.

[33] Q. Ma, H. Zhang, R. Guo, B. Li, X. Zhang, X. Cheng, M. Xie, Q. Cheng, Construction of CuS/TiO_2 nano-tube arrays photoelectrode and its enhanced visible light photoelectrocatalytic decomposition and mechanism of penicillin G, Electrochimica Acta 283 (2018) 1154–1162. https://doi.org/https://doi.org/10.1016/j.electacta.2018.07.026.

[34] M. Yan, Z. Yan, Y. Cai, B. Peng, F. Li, Efficiency and mechanism of penicillin G degradation in water by O_3/H_2O_2 method, Chinese Journal of Environmental Engineering 14(9) (2020) 2485–2493. https://doi.org/10.12030/j.cjee.202001111.

[35] L.A. Perea, R.E. Palma-Goyes, J. Vazquez-arenas, I. Romero-Ibarra, C. Ostos, R.A. Torres-Palma, Efficient cephalexin degradation using active chlorine produced on ruthenium and iridium oxide anodes : Role of bath composition, analysis of degradation pathways and degradation extent, Sci. Total Environ. 648 (2019) 377–387. doi:10.1016/j.scitotenv.2018.08.148.

[36] R. E. Palma-Goyes, J. Vazquez-Arenas, C. Ostos, F. Ferraro, R. A. Torres-Palma, I. Gonzalez, Microstructural and electrochemical analysis of Sb_2O_5 doped-Ti/RuO_2-ZrO_2 to yield active chlorine species for ciprofloxacin degradation. Electrochimica Acta 213 (2016) 740–751. https://doi.org/10.1016/j.electacta.2016.07.150

[37] I. Sirés, E. Brillas, M.A. Oturan, M.A. Rodrigo, M. Panizza, Electrochemical advanced oxidation processes: Today and tomorrow. A review, Environ. Sci. Pollut. Res. 21 (2014) 8336–8367. doi:10.1007/s11356-014-2783-1.

[38] C.D.N. Brito, D.M. De Araújo, C.A. Martínez-Huitle, M.A. Rodrigo, Understanding active chlorine species production using boron doped diamond films with lower and higher sp3/sp2 ratio, Electrochem. Commun. 55 (2015) 34–38. doi:10.1016/j.elecom.2015.03.013.

[39] G.O.S. Santos, K.I.B. Eguiluz, G.R. Salazar-Banda, C. Sáez, M.A. Rodrigo, Understanding the electrolytic generation of sulfate and chlorine oxidative species with different boron-doped diamond anodes, J. Electroanal. Chem. 857 (2020) 113756. doi:10.1016/j.jelechem.2019.113756.

[40] I. Sirés, E. Brillas, M.A. Oturan, M.A. Rodrigo, M. Panizza, Electrochemical advanced oxidation processes: Today and tomorrow. A review, Environ. Sci. Pollut. Res. 21 (2014) 8336–8367. doi:10.1007/s11356-014-2783-1.

[41] P. Cañizares, C. Sáez, A. Sánchez-Carretero, M.A. Rodrigo, Synthesis of novel oxidants by electrochemical technology, J. Appl. Electrochem. 39 (2009) 2143–2149. doi:10.1007/s10800-009-9792-7.

[42] D. Dimitrakopoulou, I. Rethemiotaki, Z. Frontistis, N.P. Xekoukoulotakis, D. Venieri, D. Mantzavinos, Degradation, mineralization and antibiotic inactivation of amoxicillin by UV-A/TiO_2 photocatalysis, J. Environ. Manage. 98 (2012) 168–174. doi:10.1016/j.jenvman.2012.01.010.

[43] S. D. Jojoa-Sierra, J. Silva-Agredo, E. Herrera-Calderon, R. A. Torres-Palma, Elimination of the antibiotic norfloxacin in municipal wastewater, urine and seawater by electrochemical oxidation on IrO_2 anodes. Sci Total Environ. 575 (2017) 1228–1238. https://doi.org/10.1016/j.scitotenv.2016.09.201

[44] E.A. Serna-Galvis, A.L. Giraldo-Aguirre, J. Silva-Agredo, O.A. Flórez-Acosta, R.A. Torres-Palma, Removal of antibiotic cloxacillin by means of electrochemical oxidation, TiO_2 photocatalysis, and photo-Fenton processes: analysis of degradation pathways and effect of the water matrix on the elimination of antimicrobial activity, Environ. Sci. Pollut. Res. 24 (2017) 6339–6352. doi:10.1007/s11356-016-6257-5.

[45] A. Zuorro, M. Fidaleo, M. Fidaleo, R. Lavecchia, Degradation and antibiotic activity reduction of chloramphenicol in aqueous solution by UV/H_2O_2 process. J. Environ Manag, 133 (2014) 302–308. https://doi.org/10.1016/j.jenvman.2013.12.012

[46] P. Villegas-Guzman, S. Oppenheimer-Barrot, J. Silva-Agredo, R. A. Torres-Palma, Comparative evaluation of photo-chemical AOPs for ciprofoxacin degradation: elimination in natural waters and analysis of pH effect, primary degradation by-products, and the relationship with the antibiotic activity. Water, Air, & Soil Pollution, 228 (2017) 209. https://doi.org/10.1007/s11270-017-3388-3

[47] A. L. Giraldo, E. D. Erazo-Erazo, O. A Flórez-Acosta, E. A. Serna-Galvis, R. A. Torres-Palma, Degradation of the antibiotic oxacillin in water by anodic oxidation with Ti/IrO_2 anodes: evaluation of degradation routes, organic by-products and effects of water matrix components. Chem Eng J. 279 (2015) 103–114. https://doi.org/10.1016/j.cej.2015.04.140

[48] C. Sarangapani, D. Ziuzina, P. Behan, D. Boehm, B. F. Gilmore, P. J. Cullen, P. Bourke, Degradation kinetics of cold plasma-treated antibiotics and their antimicrobial activity. Scientific Reports, 9 (2019) 1–15. https://doi.org/s41598-019-40352-9